CHAPTER VII

SURFACE-MODIFIED POLYMERIC FILMS BY RHAMNOLIPID BIOSURFACTANT FROM *Pseudomonas aeruginosa* SP4 FOR BIOMEDICAL APPLICATIONS

7.1 Abstract

A rhamnolipid biosurfactant extracted from the liquid culture of *Pseudomonas aeruginosa* SP4 was used to modify the surface characteristics of two types of polymeric films, including regenerated silk fibroin and chitosan, via the adsorption process. The adsorption behavior of the biosurfactant onto both polymeric surfaces was studied using the surface plasmon resonance analysis and the quartz crystal microbalance with dissipation monitoring. The water contact angles of the silk fibroin and the chitosan films after the biosurfactant adsorption were found to increase; however, the surface probe microscopy revealed that the adsorbed biosurfactant layer did not affect the surface topographies of both substrates in terms of the surface roughness. The biocompatibilities of the surface-modified polymeric films to human dermal fibroblasts and keratinocytes were investigated. Compared to the unmodified substrates, the fibroblasts grew well on the surface-modified chitosan film, but the cell growth on the surface-modified silk fibroin film was reduced. On a contrary, the surface modification of these two polymeric films did not statistically influence the growth of the keratinocytes.

Keywords: Surface modification; Biosurfactants; Rhamnolipids; Silk fibroin; Chitosan

7.2 Introduction

Much effort has been used to design, synthesize, and fabricate materials with good mechanical properties, durability, and functionality. Although all of these

properties are governed by the bulk structure, the interaction at the outermost surface, or the interface, can directly affect the utilization of the materials. For example, in biomedical applications, the biological media, cells, and tissues *in vivo* are in contact with implant surfaces, so the biointeraction, or the bioresponse, is mainly controlled by the surface characteristics of the materials, such as surface topography [1,2,3], surface wettability [4,5,6], surface chemistry [7,8,9], surface charge [10,11,12], and surface rigidity [13,14]. To get the desired properties without losing the key physical characteristics, the materials are surface-modified by using biological, mechanical, or physicochemical methods [15]. The surface modification can be divided into two main categories: chemically or physically altering the atoms, compounds, or molecules in the existing surface; and, coating the existing surface with a material having a different composition [15].

During the past few decades, both synthetic surfactants and biosurfactants have been used to modify the surface characteristics of materials via the adsorption process. Fundamentally, surface-active agents tend to adsorb at the interface in an oriented fashion [16], and an adsorbed surfactant layer can subsequently modify substratum surfaces. Jansen *et al.* [17] modified the surface characteristics of alumina particles with Triton X-100, or *t*-octylphenol poly(oxyethylene), to investigate the potential use of the modified particles as drug carriers. Amiji and Park [18] used Pluronics®, a family of triblock nonionic synthetic surfactants containing poly(ethylene oxide) (PEO) and poly(propylene oxide) (PPO), to modify the surfaces of dimethyldichlorosilane-treated glass and LDPE. The study showed that a Pluronics®-treated surface significantly prevented the platelet adhesion. Velraeds *et al.* [19] adsorbed the biosurfactant produced by *Lactobacillus acidophilus* RC14 onto the surfaces of glass and silicone rubber to reduce microbial adhesion. Rodrigues *et al.* [20] reported that the surface wettability of silicone rubber was modified after treated with the biosurfactant from *Streptococcus thermophilus* A.

In the present work, the rhamnolipid biosurfactant extracted from the liquid culture of *Pseudomonas aeruginosa* SP4 was used to modify the surface characteristics

of two types of biopolymers, including regenerated silk fibroin and chitosan, via the adsorption process. The cytotoxicities of the surface-modified polymeric substrates were also studied. Figure 7.1 shows the general chemical structures of rhamnolipid biosurfactants, silk fibroin, and chitosan. Silk fibroin and chitosan were chosen due to their potential use in biomedical applications. The silk fiber produced by the silkworm *Bombyx mori* has been commercially used as a suture for decades. After the removal of silk sericin, a glue-like protein in the raw silk fiber, the remaining material—silk fibroin—shows good biocompatibility [21] and biodegradability [22–24]. In addition, a number of cells—L929 cells [21,25], endothelial cells [26], keratinocytes, osteoblasts [27], fibroblasts [28], and bone marrow stromal cells [29]—have been shown to grow well on its surface. Chitosan is a deacetylated derivative of chitin, which is the second most plentiful biopolymer, next to cellulose. Both chitin and chitosan have drawn attention as functional polysaccharides due to their biocompatibilities [30], and recent developments have enabled their utilizations in the biomedical and veterinary fields [21, 31–34]. Chitosan is a good candidate for a surgical use as an implant for the repair of wounded skin, nerve, cartilage, and bone [30]. The adsorption of the rhamnolipid biosurfactant onto the surfaces of silk fibroin and chitosan might create suitable surface structures for therapeutic purposes, thus further expanding their potential use in the biomedical applications. Knowledge about the bioresponse could perhaps be helpful for designing tissue engineering materials.

7.3 Experimental

7.3.1 Materials

The raw silk fibers of *B. mori* were obtained from Queen Sirikit Sericulture Center (Thailand). The shells of *Penaeus merguiensis* shrimps were kindly provided by Surapon Foods Public Co., Ltd. (Thailand). Phosphate buffered saline (PBS) was supplied by Sigma-Aldrich (USA). All chemicals were used as received without further purification.

7.3.2 Preparation of Rhamnolipid Biosurfactants

P. aeruginosa SP4 was isolated from petroleum-contaminated soil in Thailand [35]. The isolated strain was maintained on nutrient agar slants at 4°C to minimize the biological activity, and was subcultured every month. To produce a biosurfactant, an inoculum was prepared by transferring the bacterial colonies into a nutrient broth, and the culture was incubated at 37°C in a shaking incubator at 200 rpm for 22 h. Then, a nutrient broth containing 2% inoculum and 2% palm oil was incubated at 37°C under aerobic conditions in a shaking incubator at 200 rpm for 48 h to obtain the highest microbial and biosurfactant concentrations [35]. The culture medium was centrifuged at 4°C and 8500 rpm for 20 min to remove the bacterial cells. The supernatant was further treated by acidification to pH 2.0 using a 6 M HCl solution, and the acidified supernatant was left overnight at 4°C for complete precipitation of the biosurfactant [36]. After centrifugation, the precipitate was removed and was dissolved in a 0.1 M $NaHCO_3$, followed by the biosurfactant extraction step with a solvent having a 2:1 CH_3Cl-to-C_2H_5OH ratio at room temperature [37]. The organic phase was transferred to a round-bottom flask connected to a rotary evaporator in order to remove the solvent. After solvent evaporation at 40°C, about 5.2 grams of a viscous honey-colored biosurfactant product was extracted per liter of the culture medium. The chemical structure of the predominant component in the biosurfactant product was identified as monorhamnolipid (Rha–C_{10}–C_{10}) (73.5%), while the others were characterized as Rha-Rha-C_8-C_{10} (0.7%), Rha-C_8-C_{10} (1.5%), Rha-C_{10}-$C_{12:1}$ (9.5%), Rha-C_{10}-C_{12} (13.3%), and Rha-Rha-C_{10}-$C_{14:1}$ (1.4%) with small contributions of their structural isomers [38]. An average molecular weight of the biosurfactant product was about 513 Da.

To prepare the biosurfactant solution, a specific amount of the biosurfactant was dissolved in the PBS solution (pH 7.4) to any desired concentrations before being vortexed to get a homogeneous solution. The sample was left at room temperature for a day to ensure equilibration before taken for the adsorption and the surface modification experiments.

7.3.3 Preparation of Polymeric Substrates

7.3.3.1 Preparation of Regenerated Silk Fibroin Film

The silk fibroin solution was prepared according to the work of Wongpanit *et al.* [39]. The raw silk fibers of *B. mori* were first boiled in a 0.05% (w/v) Na_2CO_3 solution for 15 min, followed by a thorough rinse with hot water. The boiling step, or the degumming process, was repeated two times to remove silk sericin, a family of glue-like proteins in the raw silk fibers. The degummed silks were dried at 40°C overnight before dissolving in a solvent having a 1:2:8 $CaCl_2$-to-C_2H_5OH-to-H_2O molar ratio at 78°C. The solution was dialyzed against distilled water for 4 days with a daily change of dialyzed media. The dialyzed solution was centrifuged at 10,000 rpm for 10 min before holding at 4°C. The concentration of the as-prepared silk fibroin solution was about 4.5% (w/v) before being diluted to the desired concentration. The diluted solution was then used to prepare the silk fibroin film by either the spin coating or the solvent casting technique. After the solvent was evaporated at room temperature, the obtained film was treated with a 90% (v/v) CH_3OH solution for 10 min to induce the formation of the β-sheet structure, an insoluble form of the silk fibroin. The CH_3OH-treated silk fibroin film was excessively washed with distilled water and was left to dry at room temperature.

7.3.3.2 Preparation of Chitosan Film

The preparation of chitosan from the shells of *P. merguiensis* shrimps was previously described [40]. Briefly, the shrimp shells were cleaned and then dried under sunlight before grinding into small pieces. The grinded shrimp shells were immersed in a 1 M HCl solution for 2 days with occasional stirring and were washed with distilled water until becoming neutral. The demineralized shrimp shell chips were soaked in a 4% (w/v) NaOH solution at 80–90°C for 4 h, followed by an excessive wash with distilled water. The obtained product, or chitin, was used to prepare chitosan by heating in a 50% (w/v) NaOH solution at 110°C for 1 h using an autoclave. After the deacetylation reaction, the chitosan platelets was washed with distilled water until becoming neutral and were dried at 60°C for 24 h. The viscosity-averaged molecular

weight of the chitosan product calculated from the Mark-Houwink equation [41] was about 1.1×10^6 Da. The degree of deacetylation (%DD), determined from the Fourier transform infrared (FT-IR) spectroscopy following the method of Baxter *et al.* [42], was 85.0%.

To prepare the chitosan film, a specific amount of chitosan platelets was dissolved in a 1% (v/v) CH_3COOH solution to the desired concentration. The chitosan solution was used to prepare the chitosan film by either the spin coating or the solvent casting technique. After the solvent was evaporated at room temperature, the obtained film was neutralized with a 1 M NaOH solution. The neutralized chitosan film was washed with distilled water and was left to dry at room temperature.

7.3.4 Adsorption Experiment

7.3.4.1 Surface Plasmon Resonance Analysis

The adsorption of the rhamnolipid biosurfactant onto the polymeric surfaces was studied using the SPR analysis—a well-known powerful method for measurement of thin films on the basis of an excitation of the surface plasmons by p-polarized light at the noble metal–dielectric interface [43-45]. Surface plasmons, which are electromagnetic evanescent waves, propagate along the surface with a penetration depth range of 150–200 nm [46], and the obtained SPR signal, expressed as the angle shift, is proportional to the amount of the adsorbed substance on the surface [45]. In the present work, thin films of either silk fibroin or chitosan was spun cast at the polymer concentration of 0.06% (w/v) at a speed of 1000 rpm on a glass slide coated with a 50-nm gold film. The SPR instrument (AUTOLAB, ESPRIT) was operated at room temperature. The p-polarized light was generated from a monochromatic laser light source at a wavelength of 670 nm. The flow rate across the surface during the adsorption period was 16.7 μl/s while the draining and the washing speeds were set constant at 250 μl/s. The sample injection volume was 50 μl. The SPR angle shift was reported after washing the surface with the fresh PBS solution to remove any excess biosurfactant molecules. The amount of the biosurfactant adsorbed onto the substratum surfaces was

roughly estimated from the SPR angle shift using the following relationship: a change in the SPR angle shift of 120 millidegrees (mDA) represents the adsorbed mass of 1 ng/mm^2 [47]. Dividing the adsorbed mass with an average molecular weight of the biosurfactant, the amount of the biosurfactant adsorbed onto the substratum surfaces was expressed as $\mu mol/m^2$.

7.3.4.2 Quartz Crystal Microbalance with Dissipation Monitoring

The QCM-D experiment was carried out by using a Q-sense E1 system. Prior to the measurement, the single sensor crystal with a gold coating and the rubber O-ring sealed between the sensor and the cell were cleaned by the ultrasonication in a 2% (v/v) anionic/nonionic surfactant (Decon 90) solution for 15 min. After a thorough rinse with distilled water, both the sensor and the O-ring were ultrasonicated in distilled water for 15 min before drying under a nitrogen flow. Then only the sensor was further cleaned in a UV/ozone chamber (BioForce Nanosciences, UV/Ozone ProCleaner™) for 20 min. After the cleaning process, both the sensor and the O-ring were assembled in the QCM-D instrument. The polymer solution (either silk fibroin or chitosan) at the concentration of 0.06% (w/v) was first injected into the QCM-D instrument to form a self-assembly polymer layer on the sensor surface. The weakly bound polymer molecules were removed from the sensor surface by thoroughly rinsing with a proper solvent—the distilled water (for silk fibroin) or the 1% (v/v) CH_3COOH solution (for chitosan). For the silk fibroin, the methanol treatment was also performed to induce the formation of the β-sheet structure. The biosurfactant solutions were injected at various concentrations. To remove any excess biosurfactant aggregates on the polymer layer, the fresh PBS solution was subsequently injected into the QCM-D instrument after the adsorption period. The flow rate of the test sample was set constant at 0.1 ml/min, and the temperature was controlled at 25°C. After excluding the amount of the pre-adsorbed polymer layer, the amount of the adsorbed biosurfactant was calculated from a change in the third overtone of the resonance frequency by applying the Sauerbrey equation using the software provided with the instrument. However, the mass obtained from the QCM-D technique also includes the amount of the solvent

bound to the adsorbed layer; therefore, the adsorbed mass determined from the QCM-D is always much higher than that measured by other analytical techniques, including the SPR analysis [48]. In the present work, the adsorbed masses obtained from both the QCM-D experiment and the SPR analysis were combined to get the quantitative information about the degree of hydration of the adsorbed layer on the studied substratum surfaces using the following equation:

$$\text{Water Content (\%)} = \frac{(\Gamma_{QCM-D} - \Gamma_{SPR})}{\Gamma_{QCM-D}} \times 100$$

where Γ_{QCM-D} and Γ_{SPR} are the adsorbed masses obtained from the QCM-D experiment and the SPR analysis, respectively.

7.3.5 Surface Modification of Polymeric Substrates

The polymeric substrate (either silk fibroin or chitosan film) was immersed in the biosurfactant solution at the desired concentration at room temperature for 24 h. After that, the polymeric substrate was repeatedly rinsed with the PBS solution to remove any excess biosurfactant molecules on the substratum surfaces. The surface-modified substrate was dried under a nitrogen flow before being analyses.

7.3.6 Surface Characterization of Polymeric Substrates

7.3.6.1 Water Contact Angle Measurement

The contact angle formed between the 30-μl water drop and the polymeric surface was measured by a drop shape analysis system (Krüss, DSA10 Mk2). The contact angle measurements were carried out at room temperature using the sessile drop technique. The reported values were averages of at least three measurements made at different places of the test surfaces.

7.3.6.2 Surface Probe Microscopy

The surface topography of the polymeric substrates was investigated by using a scanning probe microscope (SPM) (Veeco, Nanoscope IV) with

the tapping mode in air at room temperature. The obtained micrographs were minimally flattened, and high frequency noise was diminished in order to facilitate data analysis.

7.3.7 Cytotoxicity Tests

The cytotoxicity tests of both unmodified and surface-modified polymeric films against human dermal fibroblasts and keratinocytes were carried out at bioassay laboratory, National Center for Genetic Engineering and Biotechnology (BIOTEC), National Science and Technology Development Agency (NSTDA), Thailand. Both types of cells were grown in Dulbecco's Modified Eagle's Medium (DMEM) with 10% (v/v) of fetal bovine serum, 2 mM of L-glutamine, 100 unit/ml of penicillin, and 100 μg/ml of streptomycin. The cell cultures were incubated at 37°C in a fully humidified air atmosphere with 5% of CO_2. When the cells reached 80% confluence, they were serially sub-cultured and only the cells from the fifth passage were used.

Either unmodified or surface-modified polymeric substrate was first prepared in a well of the 24-well plate. The cells were seeded at a density of 10,000 cells/well, and were incubated at 37°C and 5% of CO_2 for the desired time interval. For the fibroblasts, the cytotoxicity was examined using the resazurin assay, the fluorescent-dye based technique [49]. After the cells were cultured for 24 h, 100 μl of the resazurin dye solution at the concentration of 62.5 μg/ml was added to each culture well. The fluorescent signal was measured everyday for 3 days at the excitation stage of 530 nm and the emission stage of 590 nm using the multi-detection microplate reader (Molecular Devices, SpectraMax M5). For the keratinocytes, the experiment was performed using the methyltetrazolium (MTT) assay; a tetrazolium-dye based colorimetric microtitration [50]. The cytotoxicity was examined after the cells were cultured for 1 day and 7 days. Briefly, the MTT solution at the concentration of 5 mg/ml was added into each well before being further incubated for 4 h. The culture medium containing the MTT solution was then removed, and the formazan crystals were solubilized in a dimethylsulfoxide (DMSO) solution. The optical density of the formazan solution was measured at the wavelength of 570 nm using the multi-detection microplate reader (Molecular Devices,

SpectraMax M5). The cells cultured in the absence of polymeric substrates were served as the control. The morphology of the cells attached on the substratum surfaces was also observed under an optical light microscope.

7.3.6 Statistical Analysis

The experimental data are presented in terms of arithmetic averages of at least three replicates, and the standard deviations are indicated by the error bars. The analyses were done using SigmaPlot software, version 8.02 (SPSS Inc., UK).

7.4 Results and Discussion

7.4.1 Adsorption of Rhamnolipid Biosurfactant

The adsorption of the rhamnolipid biosurfactant onto two types of polymeric films was investigated using the SPR analysis in a combination with the QCM-D technique. The amount of the adsorbed biosurfactant on the studied surface was reported after removing any excess biosurfactant aggregates on the pre-adsorbed polymer layer. The biosurfactant produced by *P. aeruginosa* SP4 self-assembled to form the vesicular structure in the PBS solution at the concentration above its critical micelle concentration (CMC) [51], so it was possible that the biosurfactant vesicles were also adsorbed onto the substratum surfaces, regardless of other well-ordered structures such as monolayer and bilayer. However, the adsorbed vesicles were not stable, and could be removed during the washing step. It was reported that the phospholipid liposomes adsorbed on the gold surface were removed after the rinsing process, and the remaining adsorbed phospholipid layer was resistant to further rinsing [52].

Figure 7.2 shows the adsorption isotherms of the biosurfactant onto either silk fibroin or chitosan films obtained from the two different techniques: the SPR and the QCM-D. The amount of the biosurfactant adsorbed on both polymeric substrates increased with increasing the biosurfactant concentration before reaching the plateau regions at the biosurfactant concentration above its CMC which was about 0.4 mM [38,

51]. From the SPR angle shift, the adsorbed mass of the biosurfactant onto the silk fibroin film was 4.4 μmol/m^3. Based on the assumption of bilayer topography, a surface area per molecule of 74.1 Å^2 was obtained. For the chitosan, the adsorbed mass of the biosurfactant was 2.4 μmol/m^3. Based on the assumption of monolayer topography, this value corresponded to a surface area per molecule of 71.4 Å^2. A difference in the structure of the biosurfactant molecules adsorbed onto these two polymeric films will be further discussed. The calculated surface area per molecule of the biosurfactant was close to that at the air-water interface obtained from the surface tension curve which was about 77.1 Å^2 [51].

As shown in Figure 7.2b, the adsorbed mass determined from the QCM-D technique was higher than that obtained from the SPR technique, because it included the amount of the solvent bound to the adsorbed layer on the sensor surface. From the SPR results, the adsorbed mass of the biosurfactant on the silk fibroin film was higher than that on the chitosan film. In contrast, the QCM-D results showed the opposite trend. From the QCM-D results, it seemed that the rhamnolipid biosurfactant adsorbed onto the chitosan film more than onto the silk fibroin film. However, as mentioned above, the QCM-D mass included the mass of the solvent bound to the adsorbed layer—both the polymeric films and the biosurfactant layer. Therefore, a higher adsorbed mass on the chitosan was expected to correspond to a higher amount of the adsorbed solvent, or the water in this case. Figure 7.3 shows the changes in the third overtone of the resonance frequency and the dissipation from the QCM-D experiment as a function of the biosurfactant concentration. It is known that the third overtone is much more sensitive to the region close to the surface than the fundamental frequency [53]. While the resonance frequency relates to the adsorbed mass, including the bound solvent; the dissipation factor corresponds to the thickness and the viscoelasticity of the adsorbed layer [47, 52]. As shown in Figure 7.3, the QCM-D dissipation values suggest a greater swelling of the adsorbed layer in the case of the adsorption of the biosurfactant onto the chitosan, perhaps because the chitosan adsorbed water better than the silk fibroin.

Figure 7.4 shows the water content percentages within the adsorbed layers of either silk fibroin or chitosan films as a function of the biosurfactant concentration. The results indicated that the water content within the adsorbed layer of the chitosan was higher than that of the silk fibroin at all studied biosurfactant concentrations. At the low biosurfactant concentration (lower than the CMC), the amount of the water bound to the polymer layer mainly contributed to the adsorbed mass determined from the QCM-D technique. However, the amount of the adsorbed biosurfactant increased with increasing the biosurfactant concentration. Hence, the amount of the adsorbed biosurfactant finally overcame the contribution from the adsorbed water, subsequently leading to a reduction of the water content percentages as the biosurfactant concentration increased before reaching the adsorption saturation. The high water content percentages within the adsorbed layers of either silk fibroin or chitosan films (more than 90%) further suggest that the adsorbed biosurfactant at the solid-liquid interface should possess an extended chain conformation.

In the present study, the silk fibroin was treated with an aqueous methanol solution to induce the conformation transition from random coil to β-sheet structure, which is a water-stable structure. In addition, the silk fibroin was also found to become denser after the methanol treatment, because of the shrinkage [54]. As a result, the water was difficult to bind to the silk fibroin layer. Hence, the amount of the water adsorbed onto the silk fibroin layer was lower than that onto the chitosan, subsequently leading to a lower QCM-D adsorbed mass. For the chitosan, in the present work, the chitosan was not further treated with any crosslinking agents, so its structure could interact with the water much more freely, resulting in the swelling of the chitosan layer. Our findings were also supported by the previous studies [55-57]. The degree of swelling of the methanol-treated silk fibroin was reported to be about 50% [55], while that of the chitosan was more than 100% [56, 57]. Another important aspect was that the biosurfactant molecules might probably interact with the polymeric substrates not only at the interface but also within the polymer layer in the QCM-D experiment, due to a swelling of the polymeric films, especially in the case of the chitosan.

7.4.2 Surface Characterization of Polymeric Films

It is known that the WCA is very sensitive to the structure and the chemical state of the outermost few angstroms of a surface [58], so the WCA measurement can provide useful information on the arrangement of the surfactant molecules adsorbed on the studied surface [59]. As shown in Figure 7.5, the WCAs of the silk fibroin and the chitosan films increased with increasing the biosurfactant concentration before remained stable at the biosurfactant concentration greater than its CMC. An increase in the WCA implied an increase in the amount of the biosurfactant adsorbed onto the polymeric films with the closer packing, while the steady WCA indicated that the adsorption of the biosurfactant onto the silk fibroin and the chitosan films reached saturation regions. Although the WCAs of both polymeric substrates were found to increase after the biosurfactant adsorption, they did not exceed 90°, indicating that the surfaces of both silk fibroin and chitosan films were still hydrophilic. The WCA results imply that the adsorbed biosurfactant molecules should orient with their polar head groups, their hydrophilic moieties, predominantly away from the surfaces of both polymeric substrates.

Since the biosurfactant adsorption onto both the silk fibroin and the chitosan films reached the saturation at the biosurfactant concentration greater than its CMC, the surface modification experiment was further done at the biosurfactant concentration of 2 mM, or 5 times the CMC. Figure 7.6 shows the SPM micrographs of the silk fibroin and the chitosan films before and after the biosurfactant adsorption. The surface roughness (R_a) of the unmodified silk fibroin and chitosan films determined from the SPM technique were 2.0 ± 1.0 nm and 1.4 ± 0.2 nm, respectively. After the biosurfactant adsorption, the surface-modified silk fibroin and chitosan films showed the R_a of 2.7 ± 1.5 nm and 1.6 ± 0.3 nm, respectively. The results showed that the unmodified and the surface-modified polymeric films were not statistically different in terms of the surface topography, implying that the adsorbed biosurfactant molecules should form a continuous film on the studied surfaces.

Compared between the two polymeric substrates, the surface of the silk fibroin film was rougher than that of the chitosan film, perhaps because of the self-assembly behavior of the silk fibroin. Figure 7.1b displays the chemical structure of the silk fibroin. The silk fibroin consists of at least heavy and light chains of polypeptides of approximately 350 and 25 kDa, respectively, linked by a disulfide bond at the C-terminus of the two subunits [60, 61]. The sequence of amino acids along the heavy polypeptide chain divides the silk fibroin protein chain into hydrophilic and hydrophobic blocks including ten small hydrophilic internal blocks, eleven internal hydrophobic blocks, and large hydrophilic blocks at the chain ends. The pattern of hydrophilic and hydrophobic blocks causes the silk fibroin molecules to form the micellar structures in the water, resulting in the presence of the globular structures on the silk fibroin surface after stabilized with an aqueous methanol solution [60]. These small globular structures should correspond to the surface roughness of the silk fibroin film.

Based on the SPR results, the biosurfactant molecules should adsorb onto the silk fibroin in the form of the bilayer structure, indicating that the biosurfactant molecules contacted with the surface of the silk fibroin film with their polar head group. As shown in Figure 7.1a, the rhamnolipid biosurfactant is composed of one or two molecules of rhamnose linked to one or two molecules of 3-hydroxy fatty acid. The hydrophilic head group is the rhamnose ring and the carboxylic group, while the hydrophobic tail is the fatty acid side chains. At pH 7.4, some of the rhamnolipid molecules and some of the amino acids in the silk fibroin are negatively charged due to the ionic dissociation equilibrium [62, 63]. However, the silk fibroin was weakly negative, because several amino acids in the silk fibroin were still neutral. Therefore, the effect of the electrostatic repulsion could be neglected, and the adsorption of the biosurfactant onto the silk fibroin film should occur via the hydrogen bond forming between the amide linkages in the backbone of the silk fibroin chains and the hydrophilic part of the biosurfactant. In addition, the WCA also showed that the surface of the silk fibroin film was quite hydrophilic, so the orientation of the adsorbed biosurfactant with their polar head group contacted the silk fibroin surface was favored.

Due to the hydrophobic interaction, more biosurfactant molecules were able to adsorb on the top of the first monolayer and subsequently formed the bilayer structure.

For the chitosan, the SPR results indicated that the adsorbed biosurfactant formed the monolayer structure on the surface of the chitosan film while the WCA measurement showed that the adsorbed biosurfactant molecules should orient with their polar head groups predominantly away from the substratum surfaces. Chitosan is a derivative of chitin, which is a polysaccharide, composed of D-glucosamine units and N-acetyl-D-glucosamine units joined together through glycosidic linkages. After the deacetylation reaction of chitin, most of the acetamido groups present in the chemical structure of chitin are changed to amino groups, and chitosan is achieved. Figure 7.1c shows the chemical structure of chitosan. Although the amino groups in the chitosan structure can be partially protonated to be positively charged [64] which might interact with the negatively-charged head group of the biosurfactant molecules, the chitosan are weakly positive at pH 7.4. Thus, the adsorption of the biosurfactant onto the chitosan film should be controlled by other factors. From the WCA measurement, the surface of the chitosan film showed low hydrophilicity, so the biosurfactant molecules perhaps adsorbed by turning their hydrophobic moieties contacted with the surface of the chitosan film. Since the rhamnolipid biosurfactant was negatively charged at pH 7.4, the formation of the bilayer structure was prohibited because of the electrostatic repulsion between the polar head groups of the adsorbed biosurfactant molecules in the first layer and those of the oncoming biosurfactant molecules.

7.4.3 Cytotoxicity Tests

After the surface modification, the cytotoxicities of the silk fibroin and the chitosan films to human dermal fibroblasts and keratinocytes were investigated. The cells grown in the absence of the polymeric substrates were served as controls.

Figure 7.7 shows the growth of the fibroblast cells on the polymeric films, compared to that of the control. With the use of the resazurin assay, the cell growth was expressed as the fluorescent intensity. The fluorescent intensity of all test samples was

found to increase with increasing the incubation time, implying that the fibroblasts were able to grow on the studied surfaces. Hence, the unmodified and the surface-modified polymeric films possessed a good cytocompatibility to the fibroblasts. Among the test samples, the unmodified silk fibroin film significantly enhanced the growth of the fibroblasts, but the surface modification of the silk fibroin film reduced the cell growth when the incubation time was longer than 24 h. For the chitosan film, it was found that the surface modification via the biosurfactant adsorption statistically increased the cell growth at the incubation time of 72 h. With the use of the optical light microscope, the morphology of the test cells was observed. At the incubation time of 72 h, the fibroblasts attached and spread well on the surfaces of all test samples with their filopodia. The cells also exhibited various shapes, including flattening, typical elongated fibroblast cell shapes, and spherical shapes (data not shown).

Figure 7.8 shows the growth of the keratinocyte cells on the polymeric films, compared to that of the control. The optical density of all tested samples increased as the incubation time increased from 1 day to 7 days, suggesting that the keratinocytes were able to grow on the investigated surfaces. Hence, the unmodified and the surface-modified polymeric films also possessed a good cytocompatibility to the keratinocytes. However, the surface modification of the polymeric substrates did not statistically affect the bioresponses of the keratinocytes. From the optical light microscope, at the incubation time of 1 day, the keratinocytes were able to attach on the surfaces of all test samples, and the cells showed spherical shapes. As the incubation time increased to 7 days, the attached keratinocytes exhibited flattening and typical elongated cell shapes (data not shown).

The rhamnolipid biosurfactant has great potential for biomedical field because of its good heat tolerance even after being submitted to autoclave sterilization [38]. The biological activities of the rhamnolipid biosurfactant were also widely studied in the recent years to observe its possible use in the skin care products, the skin treatment, and the wound healing [65-67]. It was reported that the rhamnolipid biosurfactant showed the skin irritating effect lower than the synthetic surfactant

(sodium dodecyl sulfate, or SDS) due to its milder interaction with keratin—the protein in skin. Stipcevic et al. [66] treated neonatal human fibroblasts and keratinocytes grown in the serum-containing medium with the rhamnolipid biosurfactant. The results showed that the biosurfactant was able to inhibit the proliferation of the fibroblasts, but enhanced the proliferation and the differentiation of the keratinocytes. Its effect on the keratinocytes suggests the possibility to use this surface-active agent in the skin treatment and the wound healing. Stipcevic et al. [67] applied a rhamnolipid-containing eucerin ointment on full-thickness burn wounds in rats covering with 5% of the total body surface area, and reported that the biosurfactant accelerated the wound healing process by accelerating the wound closure and by decreasing the collagen content in the wound area. The incorporation of the rhamnolipid biosurfactant to the tissue engineering materials might further expand its potential use in the biomedical fields, especially in the wound care applications, in the near future. In the present study, the results suggest that the cell growths can be affected by the adsorbed biosurfactant layer, the test cell types, and the selected tissue engineering materials.

7.5 Conclusions

The rhamnolipid biosurfactant extracted from the liquid culture of *P. aeruginosa* SP4 was used to modify the surface characteristics of silk fibroin and chitosan films via the adsorption process. The results suggest that the biosurfactant could be used as a tool for tailoring the surface characteristics of materials to achieve the desired bioresponse, such as the cell growth. The use of the rhamnolipid biosurfactant in the biomedical fields perhaps introduces this surface-active compound into high value-added applications.

7.6 Acknowledgements

7.7 References

[1] C.C. Berry, G. Campbell, A. Spadiccino, M. Robertson, A.S.G. Curtis, Biomaterials. 25 (2004) 5781.

[2] R.B. Vernon, M.D. Gooden, S.L. Lara, T.N. Wight, Biomaterials. 26 (2005) 3131.

[3] Y. Wan, Y. Wang, Z. Liu, X. Qu, B. Han, J. Bei, S. Wang, Biomaterials. 26 (2005) 4453.

[4] G. Khang, S.J. Lee, J.H. Lee, Y.S. Kim, H.B. Lee, Bio-med Mater Eng. 9 (1999) 179.

[5] Z.G. Tang, R.A. Black, J.M. Curran, J.A. Hunt, N.P. Rhodes, D.F. Williams, Biomaterials. 25 (2004) 4741.

[6] S.B Kennedy, N.R. Washburn, C.G. Simon Jr, E.J. Amis, Biomaterials. 27 (2006) 3817.

[7] P. Benerjee, D.J. Irvine, A.M. Mayes, L.G. Griffith, J Biomed Mater Res A. 50 (2000) 331.

[8] X.Z. Shu, K. Ghosh, Y. Liu, F.S. Palumbo, Y. Luo, R.A. Clark, G.D. Prestwich, J Biomed Mater Res A. 68A (2004) 365.

[9] L.Y. Santiago, R.W. Nowak, J.P. Rubin, K.G. Marra, Biomaterials. 27 (2006) 2962.

[10] R. Kapur, J. Lilien, G.L. Picciolo, J. Black, J Biomed Mater Res A. 32 (1996) 133.

[11] J.H. Lee, J.W. Lee, G. Khang, H.B. Lee, Biomaterials. 18 (1997) 351.

[12] Q. Qiu, M. Sayer, M. Kawaja, X. Shen, J.E. Davies, J Biomed Mater Res A. 42 (1998) 117.

[13] D. Choquet, D.P. Felsenfeld, M. Sheetz, Cell. 88 (1997) 39.

[14] C.-M. Lo, H.-B. Wang, M. Dembo, Y.-L. Wang, Biophys J. 79 (2001) 144.

[15] B.D. Ratner, A.S. Hoffman, in: B.D. Ratner, A.S. Hoffman, F.J. Schoen, J.E. Lemons (Eds.), Biomaterials sciences: an introduction to materials in medicine, Elsevier, Amsterdam, 2004, p. 201.

[16] M.J. Rosen, Surfactants and Interfacial Phenomena, Wiley-Interscience, New Jersey, 2004, p. 34.

[17] J. Jansen, C. Treiner, C. Vaution, F. Puisieux, Int J Pharm. 103 (1994) 19.

[18] M. Amiji, K. Park, Biomaterials. 13 (1992) 682.

[19] M.M. Velraeds, H.C. van der Mei, G. Reid, H.J. Busscher, Urology. 49 (1997) 790.

[20] L. Rodrigues, H. van der Mei, I.M. Banat, J. Teixeira, R. Oliveira, FEMS Immunol Med Mic. 46 (2006) 107.

[21] G.L. Jones, A. Motta, M.J. Marshall, A.E. Haj, S.H. Cartmell, Biomaterials 30:5376-5384

[22] Li M, Ogiso M, Minoura N (2003) Enzymatic degradation behavior of porous silk fibroin sheets. Biomaterials. 24 (2009) 357.

[23] T. Arai, G. Freddi, C. Innocenti, M. Tsukada, J Appl Poly Sci. 91 (2004) 2383.

[24] H.-J. Jin, J. Park, V. Karageorgiou, U. Kim, R. Valluzzi, P. Cebe, D.L. Kaplan, Adv Funct Mater. 15 (2005) 1241.

[25] N. Minoura, S. Aiba, Y. Gotoh, M. Tsukada, Y. Imai, J Biomed Mater Res A. 29 (1995) 1215.

[26] R.E. Unger, K. Peters, M. Wolf, A. Motta, C. Migliaresi, C.J. Kirkpatrick, Biomaterials. 25 (2004) 5137.

[27] R.E. Unger, M. Wolf, K. Peters, A. Motta, C. Migliaresi, C.J. Kirkpatrick, Biomaterials. 25 (2004) 1069.

[28] H. Yamada, Y. Igarashi, Y. Takasu, H. Saito, K. Tsubouchi, Biomaterials. 25 (2004) 467.

[29] H.-J. Jin, J. Chen, V. Karageorgiou, G.H. Altman, D.L. Kaplan, Biomaterials. 25 (2004) 1039.

[30] R.A.A. Muzzarelli, Carbohyd Polym. 76 (2009) 167.

[31] T. Mori, M. Okumura, M. Matsuurat, K. Ueno, S. Tokura, Y. Okamoto, S. Minam, T. Fujinaga, Biomaterials. 18 (1997) 947.

[32] G. Biagini, A. Bertani, R. Muzzarelli, A. Damadei, G. DiBenedetto, A. Belligolli, G. Ricotti, Biomaterials. 12 (1991) 281.

[33] T. Chandy, P. Sharma, Biomater Artif Cell Artif Organs. 18 (1990) 1.

[34] Y. Okamoto, S. Minami, A. Matsuhashi, H. Sashiwa, H. Saimoto, Y. Shigemasa, T. Tanigawa, Y. Tanaka, S. Tokura, J Vet Med Sci. 55 (1993) 743.

[35] O. Pornsunthorntawee, N. Arttaweeporn, S. Paisanjit, P. Somboonthanate, M. Abe, R. Rujiravanit, S. Chavadej, Biochem Eng J. 42 (2008) 172.

[36] M.M. Yakimov, H.L. Fredrickson, K.N. Timmis, Biotechnol Appl Biochem. 23 (1996) 13.

[37] Y. Zhang, R.M. Miller, Appl Environ Microb. 58 (1992) 3276.

[38] O. Pornsunthorntawee, P. Wongpanit, S. Chavadej, M. Abe, R. Rujiravanit, Bioresour Technol. 99 (2008) 1589.

[39] P. Wongpanit, N. Sanchavanakit, P. Pavasant, T. Bunaprasert, Y. Tabata, R. Rujiravanit, Eur Polym J. 43 (2007) 4123.

[40] T. Thanpitcha, A. Sirivat, A.M. Jamieson, R. Rujiravanti, Carbohyd Polym. 64 (2006) 560.

[41] W. Wang, S. Bo, S. Li, W. Qin, Int J Biol Macromol. 13 (1991) 281.

[42] A. Baxter, M. Dillon, K.D.A. Taylor, G.A.F. Roberts, Int J Biol Macromol. 14 (1992) 1661.

[43] P. Wagner, M. Hegner, H.-J. Güntherodt, G. Semenza, Langmuir. 11 (1995) 3867.

[44] C.E. Miller, W.H. Meyer, W. Knoll, G. Wegner, Ber Bunsenges Phys Chem. 96 (1992) 869.

[45] A.A. Levchenko, B.P. Argo, R. Vidu, R.V. Talroze, P. Stroeve, Langmuir. 18 (2002) 8464.

[46] P. Brandani, P. Stroeve, Macromolecules. 36 (2003) 9492.

[47] A. Kausaite, M. van Dijk, J. Castrop, A. Ramanavicience, J.P. Baltrus, J. Acaite, A. Ramanavicius, Biochem Mol Biol Educ. 35 (2007) 57.

[48] K. Sakai, E.G. Smith, G.B. Webber, C. Schatz, E.J. Wanless, V. Bütün, S.P. Armes, S. Biggs, J Phys Chem B. 110 (2006) 14744.

[49] J.O. Brien, I. Wilson, T. Orton, F. Pognan, Eur J Biochem. 267 (2000) 5421.

[50] J.A. Plumb, R. Milroy, S.B. Kaye, Cancer Res. 49 (1989) 4435.

[51] O. Pornsunthorntawee, O. Chavadej, R. Rujiravanit, Colloid Surface B. 72 (2009) 6.

[52] J.J.R. Stålgren, P.M. Claesson, T. Wärnheim T, Adv Colloid Interfac. 89-90 (2001) 383.

[53] D. Johannsmann, Macromol Chem Phys. 200 (1999) 501.

[54] P. Wongpanit, N. Sanchavanakit, P. Pavasant, T. Bunaprasert, Y. Tabata, R. Rujiravanit, Eur Polym J. 43 (2007) 4123.

[55] O. Malay, A. Batigün, O. Bayraktar, Int J Pharm. 380 (2009) 120.

[56] D. Baskar, T.S.S. Kumar, Carbohyd Polym. 78 (2009) 767.

[57] J. Sriupayo, P. Supaphol, J. Blackwell, R. Rujiravanit, Carbohyd Polym. 62 (2005) 130.

[58] C.D. Bain, E.B. Troughton, Y.T. Tao, J. Evall, G.M. Whitesides, R.G. Nuzzo, J Am Chem Soc. 111 (1989) 321.

[59] X. Song, P. Li, Y. Wang, C. Dong, R.K. Thomas, J Colloid Interface Sci. 304 (2006) 37.

[60] H.-J. Jin, D.L. Kaplan, Nature. 424 (2003) 1057.

[61] C.-Z. Zhou, F. Confalonieri, N. Medina, Y. Zivanovic, C. Esnault, T. Yang, M. Jacquet, J. Janin, M. Duguet, R. Perasso, Z.-G. Li, Nucleic Acids Res. 28 (2000) 2413.

[62] M. Nitschke, S.G.V.A.O. Costa, J. Contiero, Biotechnol Prog. 21 (2005) 1593.

[63] K. Tsukada, G. Freddi, N. Minoura, G. Allara, J Appl Polym Sci. 54 (1994) 507.

[64] K.Y. Lee, D.J. Mooney, Chem Rev. 101 (2001) 1869.

[65] G. Özdemir, Ö.E. Sezgin, Colloid Surface B. 52 (2006) 1.

[66] T. Stipcevic, T. Piljac, R.R. Isseroff, J Dermatol Sci. 40 (2005) 141.

[67] T. Stipcevic, A. Piljac, G. Piljac, Burns. 32 (2006) 24.

(a)

(b)

where R′ = -(CH₂)₃NHC(NH₂)₂ (arginine), (CH₂)₄NH₂ (lysine), -CH₂COOH

(aspartate), or -(CH₂)₂COOH (glutamate)

R″= -H (glycine), -CH₃ (alanine), or -CH₂OH (serine)

(c)
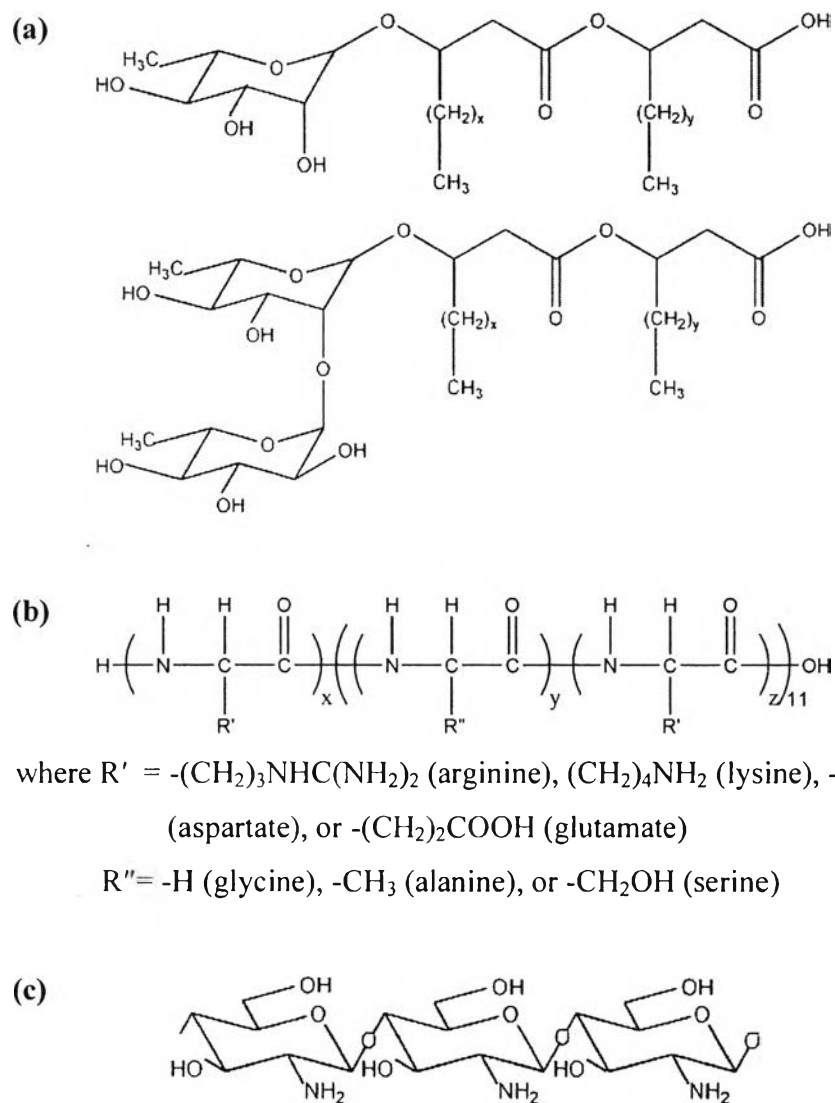
Figure 7.1 Chemical structures of (a) rhamnolipid biosurfactants, (b) silk fibroin, and (c) chitosan.
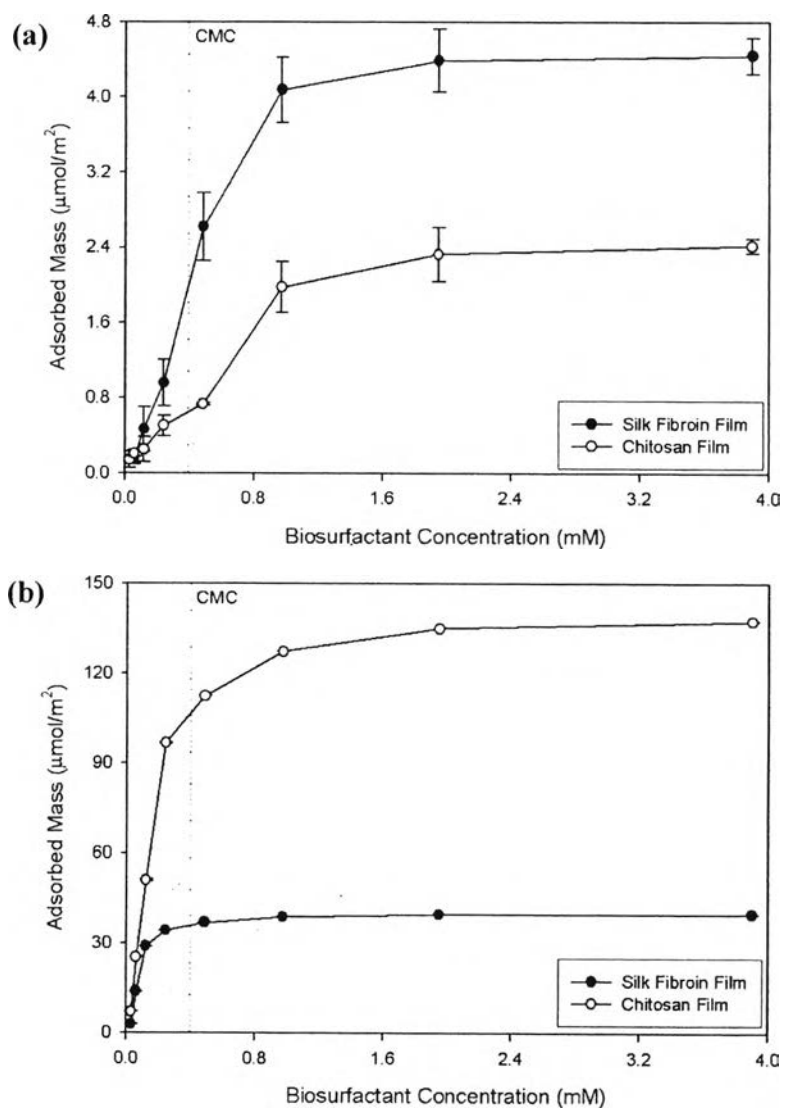
Figure 7.2 Adsorption isotherms of the rhamnolipid biosurfactant onto either silk fibroin or chitosan films from (a) the SPR analysis and (b) the QCM-D experiment.
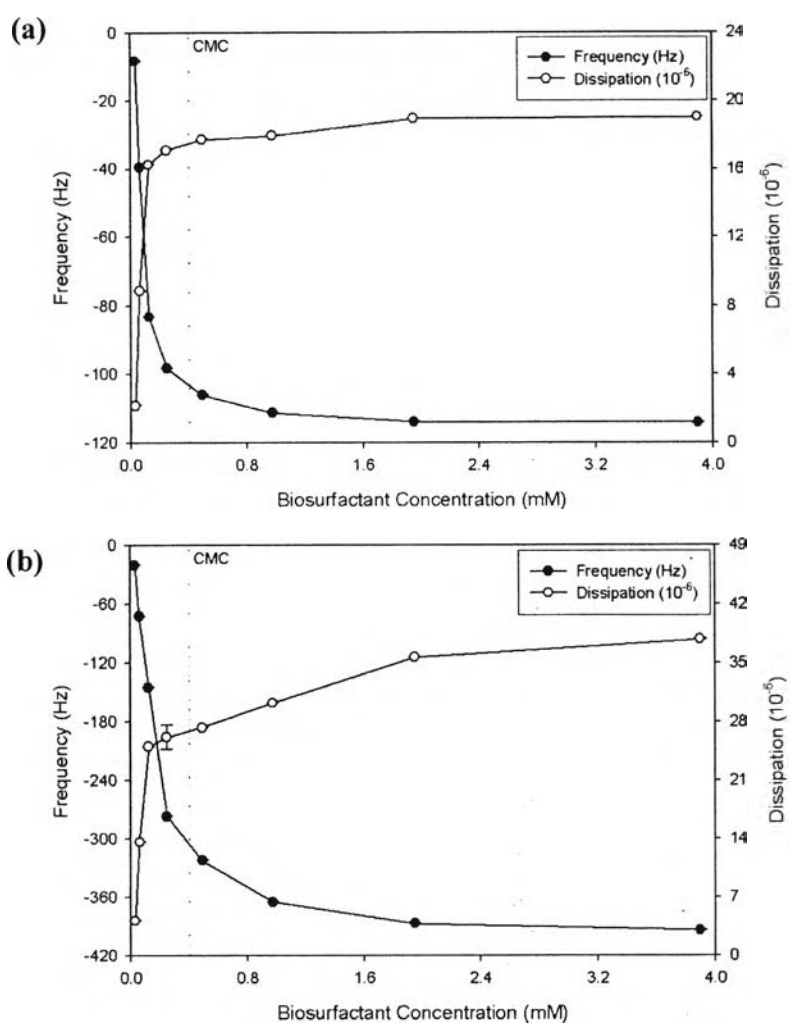
Figure 7.3 The changes in the third overtone of the resonance frequency and the dissipation from the QCM-D experiment as a function of the biosurfactant concentration: (a) silk fibroin and (b) chitosan.
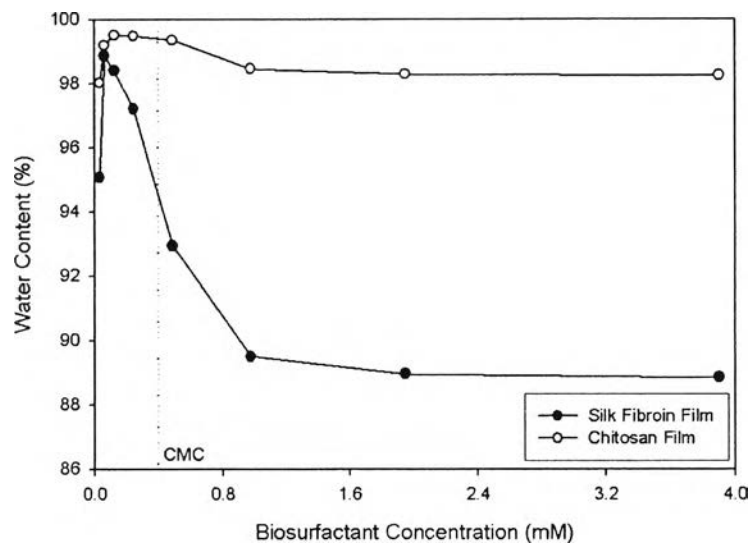
Figure 7.4 Water content percentages within the adsorbed layers of either silk fibroin or chitosan films as a function of the biosurfactant concentration.
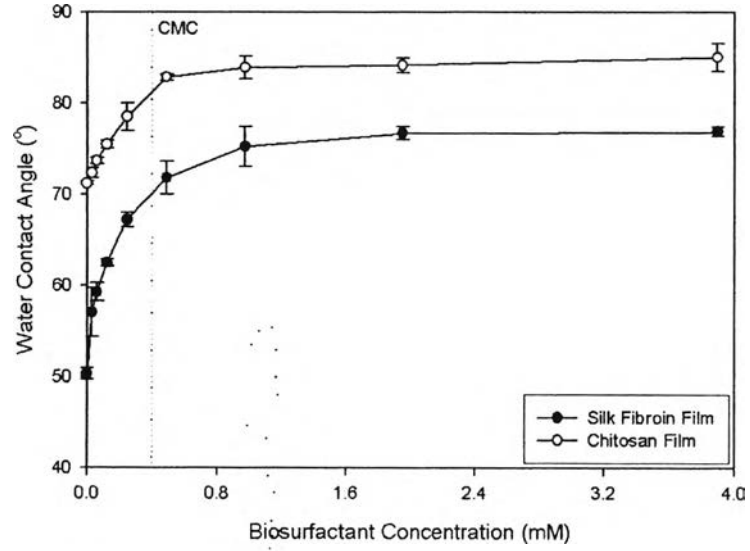
Figure 7.5 Water contact angles of either silk fibroin or chitosan films as a function of the biosurfactant concentration.
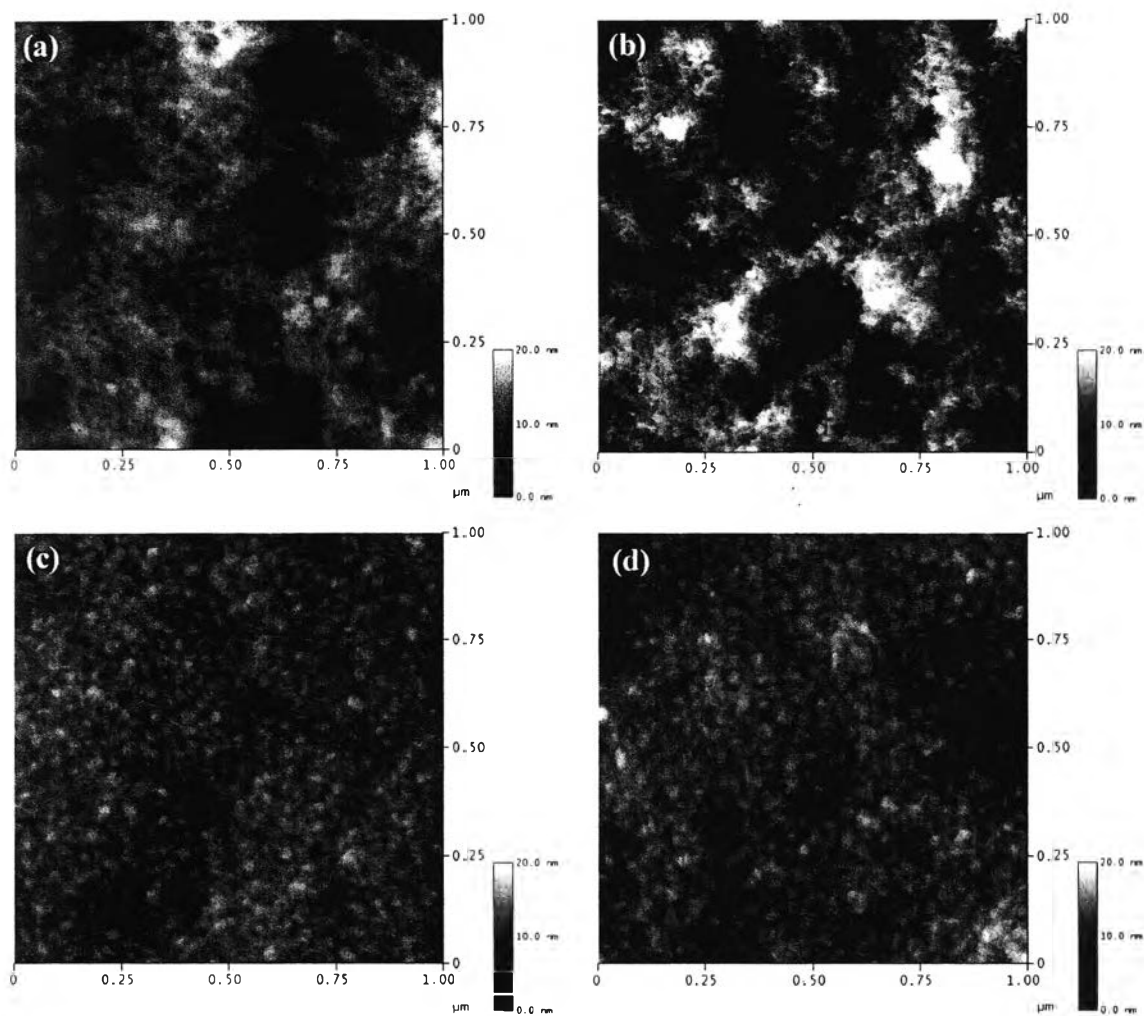
Figure 7.6 Topography AFM micrographs (scan are of 1 μm^2) of (a) unmodified silk fibroin, (b) surface-modified silk fibroin films, (c) unmodified chitosan, and (d) surface-modified chitosan.
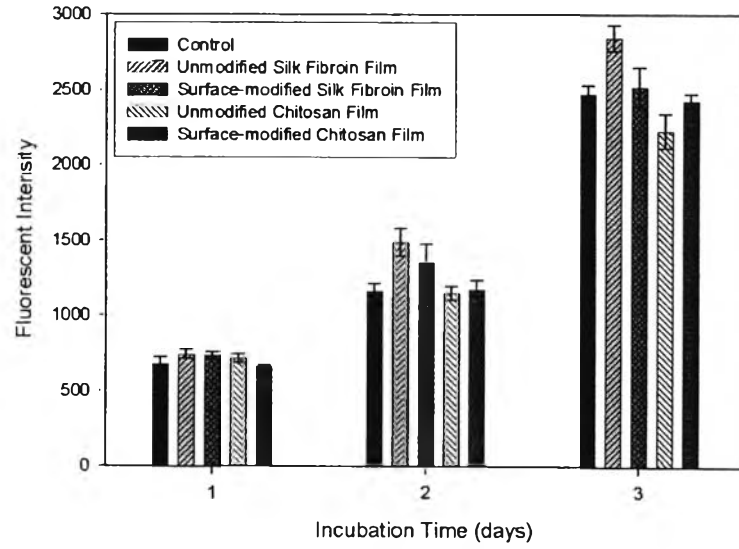
Figure 7.7 Growth of human dermal fibroblasts on unmodified and surface-modified polymeric films.
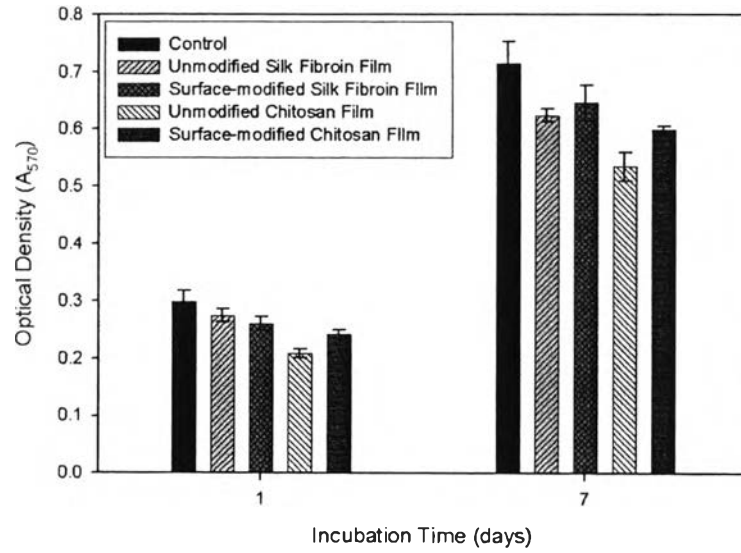
Figure 7.8 Growth of human dermal keratinocytes on unmodified and surface-modified polymeric films.